YALE PEABODY MUSEUM

JOURNAL OF MARINE RESEARCH

The *Journal of Marine Research,* one of the oldest journals in American marine science, published important peer-reviewed original research on a broad array of topics in physical, biological, and chemical oceanography vital to the academic oceanographic community in the long and rich tradition of the Sears Foundation for Marine Research at Yale University.

An archive of all issues from 1937 to 2021 (Volume 1–79) are available through EliScholar, a digital platform for scholarly publishing provided by Yale University Library at https://elischolar.library.yale.edu/.

Requests for permission to clear rights for use of this content should be directed to the authors, their estates, or other representatives. The *Journal of Marine Research* has no contact information beyond the affiliations listed in the published articles. We ask that you provide attribution to the *Journal of Marine Research.*

Yale University provides access to these materials for educational and research purposes only. Copyright or other proprietary rights to content contained in this document may be held by individuals or entities other than, or in addition to, Yale University. You are solely responsible for determining the ownership of the copyright, and for obtaining permission for your intended use. Yale University makes no warranty that your distribution, reproduction, or other use of these materials will not infringe the rights of third parties.

Anomalous diffraction approach to the visible spectra of absorption by marine particles with power-law size distributions

by Maciej Matciak[1] and Bożena Wojtasiewicz[1,2]

ABSTRACT

The spectral shape of the light absorption by marine particles with power-law size distribution was analyzed. The anomalous diffraction approximation (ADA) in its conventional form for optically "soft" homogenous particles was used to model the absorption cross section. Based on this theory, particular formulas describing the spectral shape of absorption of an assemblage of particles were derived. Exemplary calculations were performed for particles of selected shapes (spheres, thin cylinders and disks). The results suggest that relative absorption spectra of marine particles in many cases can be approximated by a simple formula, i.e. a power function of the ratio of their imaginary part of the refractive index and the light wavelength. As long as the ADA is considered, the value of the exponent varies between 0 and 1 and depends on the particle size distribution slope, the range of particles' sizes, their shapes, and the magnitude of the refractive index. These factors also influence the accuracy of this approximation.

1. Introduction

The radiative transfer in natural waters is controlled by light attenuation (absorption and scattering) by optically active components such as dissolved (CDOM) and particulate organic matter (phytoplankton, detritus, bacteria etc.) and inorganic matter (mineral particles). Their concentrations in sea water vary and influence the magnitude of absorption and scattering coefficients, which characterize quantitatively the light attenuation, and are involved in the radiance and irradiance transport equations (e.g. Jerlov, 1976; Thomas and Stamnes, 1999). The irradiance decay in the water column depends directly on the magnitude of the absorption coefficient, whereas a water body's diffusive reflectance is determined by the relationship between the backscattering coefficient and absorption (Gordon *et al.,* 1975; Kirk, 1984, 1991; Mobley, 1994). Light absorption plays an essential role in photosynthesis; however, only a few percents of the available solar energy is used for this purpose. Almost all absorbed light is converted into heat (Lewis *et al.,* 1983; Dera, 2003). The absorption of visible radiant energy by marine particles can be a significant component of the sea heat budget. It can manifest itself by increases in the temperature

---

1. Institute of Oceanography, University of Gdańsk, al. Marszałka Piłsudskiego 46, 81–378 Gdynia, Poland.
2. Corresponding author. *email: bwojtasiewicz@ocean.ug.edu.pl*

within the upper mixed layer which accompany local accumulations of particulate matter (e.g. Ramp *et al.,* 1991; Stramska and Dickey, 1993; Chang and Dickey, 2004). Consequently, the light absorption influences the vertical and horizontal water density structure and probably water circulation (Simpson and Dickey, 1981; Lewis *et al.,* 1983; Edwards *et al.,* 2001, 2004; Oschlies, 2004). Increased knowledge on the absorption spectra of optically active constituents of sea water is vital for many types of research. For example, investigations of the radiant heating rate of both modeling and experimental character relate to the spectral integral describing the solar energy absorption (Ohlmann *et al.,* 2000; Chang and Dickey, 2004). Spectral information on optical signals originating from the sea water and emerging from below the sea surface is also necessary for research carried out using remote sensing (e.g. Zaneveld *et al.,* 2006).

Apart from the physical properties of individual particles, the light attenuation by marine suspended matter depends on their sizes and concentrations, which are taken into account through the particle size distribution (PSD). PSD represents the number of particles of sizes $D \pm 0.5dD$ per unit volume of water. When considering a relatively wide interval of particle sizes up to the order of 1000 μm, it is evident that the global size distribution is primarily characterized by a rapid decrease in the number of large particles. Such a distribution can be approximated by a decreasing power-law function (Bader, 1970):

$$n(D) = mD^{-k} \quad [\mathrm{m}^{-3}\mu\mathrm{m}^{-1}] \tag{1}$$

where D [μm] is a characteristic size of particles; m [$\mathrm{m}^{-3}\mu\mathrm{m}^{k-1}$] and nondimensional k are positive constants.

The power-law size distribution can often be successfully applied for particles from various water bodies (e.g. Carder *et al.,* 1971; Sheldon *et al.,* 1972; Harris, 1977; McCave, 1984, Buonassissi and Dierssen, 2010). The value of k varies between 2 and 6, but most frequently it is close to 4 (e.g. Jonasz and Fournier, 2007). In particular cases segmented power-law PSDs can be more accurate approximations. Another approach is to use a sum of generalized gamma or log-normal distributions which can account for the fact that the number of the smallest particles (with sizes usually much smaller than 1 μm) can decrease with decreasing size (Risovic, 1993; Jonasz and Fournier, 1996). However, the power-law size distribution represents a basic feature of PSDs of larger particles, which mostly contribute to the magnitude of the absorption and scattering coefficients. Therefore it is frequently applied in analyses of the influence of marine particles on the light attenuation in the ocean (Boss *et al.,* 2001; Chang *et al.,* 2007; Doxaran *et al.,* 2009; Kostadinov *et al.,* 2009).

It has been recognized that the visible spectra of scattering coefficient of assemblages of nonabsorbing spherical particles characterized by constant refractive index and power law PSD with infinite diameter size intervals $(0-\infty$ μm) can be described by a function $\lambda^{-\varepsilon}$ where λ is the light wavelength and ε is a positive exponent. The epsilon value is related to the PSD slope coefficient k (Eq. 1) in a simple way, $\varepsilon = k - 3$ for $3 < k < 7$ (Morel, 1973; Boss *et al.,* 2001; Jonasz and Fournier, 1996; Twardowski *et al.,* 2001). This result

had been known in the atmospheric physics earlier. The power wavelength dependency of aerosol light attenuation was introduced by Angstrom (1929). Then Volz (1954), who analyzed the light scattering by nonabsorbing aerosols, showed how to obtain the relationship between the exponent in the Angstrom formula and *k* by an appropriate change of variables in the expressions describing the scattering coefficient. The argument presented by Volz can also be referred to in the case of scattering by marine particles, because the description of the light attenuation processes is the same for both atmospheric and marine particles. Actually, the scattering spectra of marine particles are strongly influenced by the absorption and often they can hardly resemble a simple power function of the wavelength (e.g. Barnard *et al.,* 1998; Babin *et al.,* 2003). Nevertheless it seems that the Volz's method could be used and further explored in the case of particle absorption modeled with the use of the anomalous diffraction approximation (ADA). To our knowledge the spectral shape of marine particles' absorption characterized by the power-law PSD has never been analyzed in such a way.

Particularly in the case of polydispersive particles ADA offers a significant simplification and reasonable accuracy in calculating particulate optical attenuation in comparison to the exact methods based on Maxwell's equations, such as the commonly employed Mie or T-matrix solutions (Mishchenko *et al.,* 2002; Bohren and Huffman, 2004). Van de Hulst (1981) developed this theory in order to determine the light attenuation efficiencies of homogeneous, spherical particles. With respect to the usefulness of this approach, it has been extensively studied (see e.g. http://www.astro.spbu.ru/DOP/3-REVS/KHLEB1/). For example, some approximate and exact solutions were obtained for particles of regular shapes: spheroids (Fournier and Evans, 1994; Paramonov, 1994), very thin circular and elliptical cylinders (Fournier and Evans, 1996), and hexagons (Sun and Fu, 1999). Quirantes and Bernard (2004) also obtained solutions for nonhomogenous spherical particles, so-called coated spheres. The basis for the anomalous diffraction approximation for absorption of arbitrarily shaped particles is the general integral which determines the absorption cross section at a given particle orientation relative to the incident light (e.g., Bryant and Latimer, 1969; Liu *et al.,* 1998; Yang *et al.,* 2004):

$$C_a = \int\int_P \left[1 - \exp\left(-\frac{4\pi n_w l_p r}{\lambda} \right) \right] dP \quad [\text{m}^2] \tag{2}$$

where λ is the wavelength in the vacuum, r is the light ray path through the particle, dP is an element of the particle projected area (P) on the plane perpendicular to the direction of the light ray, n_w is the real part of the refractive index of water, and l_p is the imaginary part of the refractive index relative to water.

The ray paths are line segments within a particle whose direction is the same as the direction of the incident light. Neglecting the light refraction and reflection on a particle surface results from the basic ADA assumption that the absolute value of a particle complex index of refraction relative to the surrounding medium ($m_p = n_p - il_p$) is

close to 1; that is, its real part is close to 1 and the imaginary part is close to 0. Most marine particles fulfill this condition; i.e., n_p is lower than 1.1 (e.g. Morel, 1994; Aas, 1996) and l_p is on the order of between 10^{-4} and 10^{-2} (e.g. Bricaud and Morel, 1986; Stramski *et al.,* 2001). Moreover, despite being primarily developed for particles that are large in comparison to the light wavelength, ADA approximates well the absorption efficiencies of the smallest particles (Latimer, 1984; Morel, 1994; Jonasz and Fournier, 2007). In this case, when the refractive index is wavelength independent, this approximation predicts particle absorption coefficient spectrum ($\sim\lambda^{-1}$) exactly as the rigorous solutions. This dependency is known as the Rayleigh law for the absorption (e.g. Bohren and Huffman, 2004). Unfortunately, ADA fails in describing the spectral shape of scattering of light by small particles. It results from the ADA general formulation of the scattering cross section (e.g. Bryant and Latimer, 1969; Liu *et al.,* 1998; Yang *et al.,* 2004), that for example in the case of particles with constant complex refractive index the spectral dependency known as the Rayleigh law for the scattering cannot be obtained (e.g. Bohren and Huffman, 2004).

It should be mentioned here that Duysens (1956) independently developed an approach to the algal suspension absorption with results being equivalent to the conventional ADA (e.g., Morel and Bricaud, 1981). In Duysens' method the absorption properties of algae are expressed as a product of the intracellural pigment concentration and the specific pigment absorption coefficient, not by means of the refractive index as in Eq. 2. This approach was applied by Kirk (1975, 1976) and Baird (2003) for calculating the absorption spectra of particles of various shapes.

We expect that applying ADA will bring some fresh insight into the spectral shape of absorption by particles characterized with the power-law PSD. We will begin the analysis from the case of large particles' size ranges. Then we will derive a solution for the absorption spectra shape in the limiting case when the particle sizes expand from 0 to infinity. This solution is an important point to understand and interpret the courses of the particulate absorption spectra. Based on the obtained results, we will consider the absorption spectra of assemblages of particles with narrower size ranges which are likely to occur in the small volume samples of sea water used in laboratory measurements of the particulate absorption.

2. Theory—basic relations

For particles of the same l_p spectrum and shape but different sizes, the absorption coefficient (a_p) is described by the following formula (e.g. Jonasz and Fournier, 2007):

$$a_p(\lambda) = \int_{D_{min}}^{D_{max}} C_a n(D)dD \quad [\text{m}^{-1}] \tag{3}$$

where D is the characteristic particle size and D_{min} and D_{max} are its minimum and maximum values, respectively.

Accounting for the geometrical similarity of particles, the variations of their sizes can be described only by one dimension. In theoretical considerations the choice of this dimension usually results from the assumed particles' symmetry. In practice, measurements of size distributions of highly irregular in shape particles are usually related to the particles' volume (e.g. Coulter counter) and then the sphere volume-equivalent diameter is often considered to be the characteristic size (e.g., Jonasz and Fournier, 2007).

Substituting the expression for the absorption cross section (Eq. 2) and the power-law particle size distribution (Eq. 1) into Eq. 3, and then arranging the variable D so as to make the surface integral independent from particle size, one can obtain:

$$a_p(\lambda) = m \int_{D_{\min}}^{D_{\max}} \left\{ \iint_{P/D^2} \left[1 - \exp\left(-4\pi n_w \left(\frac{r}{D} \right) \frac{l_p}{\lambda} D \right) \right] d\left(\frac{P}{D^2} \right) \right\} D^{2-k} dD. \qquad (4)$$

The ratios r/D and P/D^2 do not depend on a particle size and thereby they are not dependent on D.

After introducing the parameter $y = l_p \lambda^{-1} D$ into Eq. 4 by substitution $D = \lambda l_p^{-1} y$ the absorption coefficient equals:

$$a_p(\lambda) = m \left(\frac{l_p}{\lambda} \right)^{k-3} \int_{y_{\min}}^{y_{\max}} \left\{ \iint_{P/D^2} \left[1 - \exp\left(-4\pi n_w \left(\frac{r}{D} \right) y \right) \right] d\left(\frac{P}{D^2} \right) \right\} y^{2-k} dy \qquad (5)$$

where $y_{\min} = l_p \lambda^{-1} D_{\min}$, $y_{\max} = l_p \lambda^{-1} D_{\max}$.

Let us write Eq. 5 for randomly oriented particles and divide both sides by the absorption coefficient for a given reference wavelength (λ_o):

$$\frac{a_p(\lambda)}{a_p(\lambda_o)} = \left(\frac{l_p}{\lambda} \right)^{k-3} \left(\frac{\lambda_o}{l_{po}} \right)^{k-3} \frac{\displaystyle\int_{y_{\min}}^{y_{\max}} \langle C_a^*(y) \rangle y^{2-k} dy}{\displaystyle\int_{y_{o\,\min}}^{y_{o\,\max}} \langle C_a^*(y_o) \rangle y_o^{2-k} dy_o} \qquad (6)$$

where $\langle C_a^* \rangle = \left\langle \int \int_{P/D^2} \left\{ 1 - \exp\left[-4\pi n_w \left(\frac{r}{D} \right) y \right] \right\} d\left(\frac{P}{D^2} \right) \right\rangle$ represents the average absorption cross section $\langle C_a \rangle$ resulting from random orientation of particles divided by D^2 and $l_{po} = l_p(\lambda_o)$, $y_{o\,\min} = l_{po} \lambda_o^{-1} D_{\min}$, $y_{o\,\max} = l_{po} \lambda_o^{-1} D_{\max}$.

Then, Eq. 6 can be rewritten in a following way:

$$\frac{a_p(\lambda)}{a_p(\lambda_o)} = \left(\frac{l_p}{\lambda}\right)^{k-3}\left(\frac{\lambda_o}{l_{po}}\right)^{k-3}\left[1 + \frac{\displaystyle\int_{y_{min}}^{y_{max}}\langle C_a^*(y)\rangle y^{2-k}dy - \int_{y_{o\,min}}^{y_{o\,max}}\langle C_a^*(y_o)\rangle y_o^{2-k}dy}{\displaystyle\int_{y_{o\,min}}^{y_{o\,max}}\langle C_a^*(y_o)\rangle(y_o)y_o^{2-k}dy}\right]. \tag{7}$$

The difference of the integrals in the Eq. 7 can be expressed as:

$$\int_{y_{min}}^{y_{max}}\langle C_a^*(y)\rangle y^{2-k}dy - \int_{y_{o\,min}}^{y_{o\,max}}\langle C_a^*(y_o)\rangle y_o^{2-k}dy$$

$$= \int_{y_{o\,max}}^{y_{max}}\langle C_a^*(y'_{max})\rangle y_{max}'^{2-k}dy'_{max} - \int_{y_{o\,min}}^{y_{min}}\langle C_a^*(y'_{min})\rangle y_{min}'^{2-k}dy'_{min} \tag{8}$$

and after changing variables from y to l_p/λ one can easily obtain:

$$\int_{y_{o\,max}}^{y_{max}}\langle C_a^*(y'_{max})\rangle y_{max}'^{2-k}dy'_{max} - \int_{y_{o\,min}}^{y_{min}}\langle C_a^*(y'_{min})\rangle y_{min}'^{2-k}dy'_{min}$$

$$= \int_{l_{po}/\lambda_o}^{l_p/\lambda}\left[\langle C_a^*(D_{max})\rangle D_{max}^{3-k} - \langle C_a^*(D_{min})\rangle D_{min}^{3-k}\right]\left(\frac{l_p}{\lambda}\right)^{2-k}d\left(\frac{l_p}{\lambda}\right). \tag{9}$$

If this formula is substituted into Eq. 7 the result is as follows:

$$\frac{a_p(\lambda)}{a_p(\lambda_o)} = \left(\frac{l_p}{\lambda}\right)^{k-3}\left\{\left(\frac{\lambda_o}{l_{po}}\right)^{k-3} + \frac{1}{\gamma_o}\int_{l_{po}/\lambda_o}^{l_p/\lambda}\left[\langle C_a^*(D_{max})\rangle D_{max}^{3-k} - \langle C_a^*(D_{min})\rangle D_{min}^{3-k}\right]\left(\frac{l_p}{\lambda}\right)^{2-k}d\left(\frac{l_p}{\lambda}\right)\right\} \tag{10}$$

where $\gamma_o = \dfrac{a_p(\lambda_o)}{m} = \int_{D_{min}}^{D_{max}}\langle C_a^*(\lambda_o)\rangle D^{2-k}dD$.

Eq. 10 describes particle absorption dependency on the wavelength in a way which is as complex as in Eqs. 3 and 4. However, the domain of integration is not related to the particles' sizes. Therefore, there is an opportunity to simplify the calculations and to obtain some useful solutions. Assuming that the minimum size of the particles is small enough to enhance using the linear approximation of the exponential function in the expression $1 - \exp\left[-4\pi n_w\left(\dfrac{r}{D}\right)\dfrac{l_p}{\lambda}D\right]$ (Eq. 6), the absorption cross section can be written as:

$$\langle C_a^*(D_{min})\rangle = \alpha\left(\frac{l_p}{\lambda}\right)D_{min} \tag{11}$$

with nondimensional coefficient $\alpha = 4\pi n_w \left\langle \int \int_{P/D^2} \left(\dfrac{r}{D_{\min}}\right) d\left(\dfrac{P}{D_{\min}^2}\right) \right\rangle$ which is characteristic for a given particles' shape for the region of $D_{\min} \to 0$.

At the same time it was assumed that the maximum diameter is so large that the absorption cross section $\langle C_a^* \rangle$ is equal to a certain nondimensional constant $\beta = \left\langle \int \int_{P/D^2} d\left(\dfrac{P}{D^2}\right) \right\rangle$ also characteristic for a given particles' shape. The product of β and D^2 is the particle mean projected area, which is the maximum value of the absorption cross section $\langle C_a \rangle$. It can be easily calculated for randomly oriented convex particles using the Cauchy theorem according to which a particle mean projected area equals ¼ of its lateral surface (e.g. Vickers and Brown, 2001).

Accounting for the above two assumptions Eq. 10 simplifies considerably:

$$\frac{a_p(\lambda)}{a_p(\lambda_o)} = \left(\frac{l_p}{\lambda}\right)^{k-3} \left\{ \left(\frac{\lambda_o}{l_{po}}\right)^{k-3} + \frac{1}{\gamma_o} \int_{l_{po}/\lambda_o}^{l_p/\lambda} \left[\beta D_{\max}^{3-k} \left(\frac{l_p}{\lambda}\right)^{2-k} - \alpha D_{\min}^{4-k} \left(\frac{l_p}{\lambda}\right)^{3-k} \right] d\left(\frac{l_p}{\lambda}\right) \right\}. \tag{12}$$

After integration three solutions were obtained depending on the value of k.

When and $k \neq 3$ and $k \neq 4$:

$$\frac{a_p(\lambda)}{a_p(\lambda_o)} = A\,\frac{l_p}{\lambda} + B\left(\frac{l_p}{\lambda}\right)^{k-3} + C \tag{13}$$

where:

$$A = -\frac{\alpha}{\gamma_o}\frac{D_{\min}^{4-k}}{4-k}, \quad B = -A\left(\frac{l_{po}}{\lambda_o}\right)^{4-k} + (1-C)\left(\frac{l_{po}}{\lambda_o}\right)^{3-k}, \quad C = \frac{\beta}{\gamma_o}\frac{D_{\max}^{3-k}}{3-k}.$$

When $k = 3$:

$$\frac{a_p(\lambda)}{a_p(\lambda_o)} = A\left(\frac{l_p}{\lambda}\right) + B\ln\left(\frac{l_p}{\lambda}\right) + C \tag{14}$$

where

$$A = -\frac{\alpha D_{\min}}{\gamma_o}; \quad B = \frac{\beta}{\gamma_o}; \quad C = 1 - A\left(\frac{l_{po}}{\lambda_o}\right) - B\ln\left(\frac{l_{po}}{\lambda_o}\right).$$

For $k = 4$:

$$\frac{a_p(\lambda)}{a_p(\lambda_o)} = A\left(\frac{l_p}{\lambda}\right) + B\left(\frac{l_p}{\lambda}\right)\ln\left(\frac{l_p}{\lambda}\right) + C \tag{15}$$

where

$$A = (1-C)\left(\frac{l_{po}}{\lambda_o}\right)^{-1} - B\ln\left(\frac{l_{po}}{\lambda_o}\right); \quad B = -\frac{\alpha}{\gamma_o}; \quad C = -\frac{\beta}{\gamma_o D_{\max}}.$$

These solutions were obtained under the assumption that all particles in an assemblage are of the same shape but without specifying their exact geometry. Therefore the general spectral dependency of the relative absorption coefficient is the same for particles of any shape. The shape of particles in a considered assemblage determines the values of α and β coefficients, which influence the magnitude of A, B, and C constants.

In order to obtain a solution describing the absorption spectra for the infinitely large particle size range, i.e. when $D_{min} \rightarrow 0$ and $D_{max} \rightarrow \infty$ limiting values of the expressions D_{min}^{4-k}/γ_o, D_{min}^{3-k}/γ_o, D_{min}/γ_o, $1/\gamma_o$, and $1/(\gamma_o D_{max})$ in Eqs. 13–15 should be used to determine the values of the coefficients A, B, and C. When calculating the limits it has to be taken into account that the magnitude of the absorption coefficient and therefore γ_o can be infinitely large. When $D_{max} \rightarrow \infty$ and $D_{min} \rightarrow 0$ the integral $\int_{D_{min}}^{D_{max}} \left\{ 1 - \exp\left[-4\pi n_w \left(\frac{r}{D}\right) \frac{l_p}{\lambda} D \right] \right\} D^{2-k} dD$ exists only for $3 < k < 4$ whereas for other values of k it is divergent. The divergence of this integral is a consequence of the behavior of the integrand when $D_{max} \rightarrow \infty$ for $k \leq 3$ or when $D_{min} \rightarrow 0$ for $4 \leq k$. These outcomes can be proved by using appropriate criteria on the convergence of improper integrals (e.g., Fichtenholz, 1978). The limiting values can be easily obtained in some cases, e.g. for $3 < k < 4$ (Eq. 13) A and C vanish and the value of the coefficient B equals $(l_{po}/\lambda_o)^{3-k}$. In other cases de l'Hopital's rule has to be used because of the presence of the indeterminate forms. For example, we present the calculation of the limit for $4 < k$ (Eq. 13):

$$\lim_{D_{min} \to 0} \frac{D_{min}^{4-k}}{\gamma_o} = -\lim_{D_{min} \to 0} \frac{(4-k)D_{min}^{3-k}}{\langle C_a^*(D_{min}, \lambda_o) \rangle D_{min}^{2-k}} = \frac{k-4}{\alpha}\left(\frac{l_{po}}{\lambda_o}\right)^{-1}. \tag{16}$$

In these calculations the limiting form of the absorption cross section when $D_{min} \rightarrow 0$ (Eq. 11) was applied. Accounting for the fact that $\lim_{D_{min} \to 0} D_{max}^{3-k}/\gamma_o = 0$ the only nonzero coefficient in Eq. 13 is $A = (l_{po}/\lambda_o)^{-1}$. After calculating all the limits and substituting their values into Eqs. 13–15 the solution (*asymptotic*) is as follows:

$$\frac{a_p(\lambda)}{a_p(\lambda_o)} = \begin{cases} 1 & \text{for } k \leq 3 \\ \left(\dfrac{l_{po}}{\lambda_o}\right)^{3-k}\left(\dfrac{l_p}{\lambda}\right)^{k-3} & \text{for } 3 < k < 4 \\ \left(\dfrac{l_{po}}{\lambda_o}\right)^{-1}\left(\dfrac{l_p}{\lambda}\right) & \text{for } 4 \leq k \end{cases}. \tag{17}$$

Thus, from the mathematical point of view it is possible to determine the absorption spectral shape in the asymptotic case, even though the values of the absorption coefficient do not exist. When the sizes of particles expand from 0 to infinity the absorption spectrum is proportional to a power function of $l_p \lambda^{-1}$ whose exponent, ranging from 0 to 1, depends on the PSD slope or, in other words, on the relationship between the number of large and fine particles (Eq.17). When the exponent equals 0 (for $k \leq 3$), the absorption spectrum is flat for any l_p spectrum. This results from the domination of large particles whose $\langle C_a \rangle$ is wavelength independent because it equals the mean projected area. When $3 < k < 4$ the exponent changes with changing value of the PSD slope, namely as $k - 3$. When the value

of the exponent equals 1 then the influence of the finest particles on the spectral shape of absorption is the most important and the wavelength dependency is the same as for the absorption Rayleigh law.

Basing on Eqs. 13–15 one can determine the absorption spectrum when $D_{max} \rightarrow \infty$ or $D_{min} \rightarrow 0$. In some cases the result will be the same as in Eq. 17, i.e. for an infinitely large D_{max} and $k \leq 3$ or $D_{min} \rightarrow 0$ and $4 \leq k$. Eqs. 13–15 can be modified when one additionally accounts for the absorption by particles of diameters lower that D_{min} $(0, D_{min})$ and different PSD, especially when the number of particles decreases when their sizes tend to 0. Since their absorption coefficient is proportional to $l_p \lambda^{-1}$ the dependency of the relative total particle absorption coefficient on $l_p \lambda^{-1}$ stays the same as given by Eqs. 13–15 but the values of the coefficients A, B, and C will change.

The solution given by Eq. 13 is a sum of three terms corresponding to appropriate asymptotic absorption spectrum (note that the last term in Eq. 13 can be written as $1 \cdot C$ and 1 is a part of solution given by Eq. 17). Depending on the k value, one of these terms can start to be dominating, because Eq. 13 is valid for a wide range of particles' sizes and consequently it can be close to the asymptotic solution which is a one-term power function. In fact, the value of D_{max} resulting from the condition for obtaining Eq. 13 can be sufficiently large when the PSD is steep enough and the contribution of the largest particles to the magnitude of the relative absorption coefficient is small. Therefore one can try to approximate Eq. 13 with a one-term power function:

$$\frac{a_p(\lambda)}{a_p(\lambda_o)} = \left(\frac{l_{po}}{\lambda_o}\right)^{-\delta} \left(\frac{l_p}{\lambda}\right)^{\delta} \tag{18}$$

where an exponent δ depends on the value of k.

This simplification relates also to the particular solutions (Eqs. 14, 15), which are the limiting cases of Eq. 13 when k tends to 3 or 4. On the other hand, according to ADA, the absorption coefficient for the smallest particles is proportional to $(l_p \lambda^{-1})^1$. So when the values of D_{max} are large or very low the approximation is a power function of $l_p \lambda^{-1}$. It can be expected, that for intermediate D_{max} values which do not fulfill the assumption of Eq. 12, the approximation of absorption spectra can also be expressed as in Eq. 18. This case is important when determining the absorption in laboratory conditions on discrete seawater samples when large particles, whose concentration is usually relatively low, can be missed during sampling. At present, such laboratory measurements are the only way to measure discriminately the absorptive properties of two main components of particulate matter, algal and nonalgal particles (e.g. Woźniak and Dera, 2007). The particulate absorption can be measured in suspension when small volumes of water (a few cm^3) are put into a cell placed inside an integrating sphere in order to eliminate the influence of scattering. This method is limited to water samples of sufficiently large particle load and cannot be used for oceanic waters. In this case the most frequently used absorption measurement methods are filter techniques (e.g. Yentsch, 1962; Mitchell, 1990; Tassan and Ferrari, 1995) which involve concentration of a certain volume of water on glass fiber filters. The volume of

filtered sea water usually does not exceed 5 L (e.g. Mitchell *et al.,* 2000). In the next sections we will investigate the validity of Eq. 18 in modeling the absorption spectra for assemblages of particles with various values of D_{max}.

3. Calculations

a. Assumptions

All calculations of relative absorption spectra were performed within the visible band (350–750 nm) for homogeneous particles of three different shapes—spheres, very thin cylinders, and disks. Because they all are solids of revolution and have a plane of symmetry, their shape can be characterized by the aspect ratio defined as the dimension (height) along the axis of rotation divided by the diameter in the symmetrical plane. Considering this parameter, cylinders and disks are the extreme shapes; i.e. for cylinders the aspect ratio is very large whereas for disks it is close to 0. It can be expected that results obtained for these limiting shapes will determine the absorption spectra variability range and the absorption properties of particles with moderate aspect ratios will be found within these limits. In turn, a sphere with the aspect ratio of 1 is the most compact shape for which majority of calculations of optical properties of particles are being performed (e.g. Bricaud and Morel, 1986; Stramski *et al.,* 2001; Woźniak and Stramski, 2004; Doxaran *et al.,* 2009).

The relative absorption coefficient $\langle C_a \rangle$ was determined on the basis of the formula in which the absorption cross section was expressed as a product of the nondimensional absorption efficiency (Q_a) and a particle mean projected area:

$$\frac{a_p(\lambda)}{a_p(\lambda_o)} = \frac{\int_{D_{min}}^{D_{max}} 0.25 S Q_a(\lambda, D) D^{-k} dD}{\int_{D_{min}}^{D_{max}} 0.25 S Q_a(\lambda_o, D) D^{-k} dD} \tag{19}$$

where D is a characteristic particle size, D_{min} and D_{max} are the minimum and maximum of D, respectively and S is the particle surface.

We assumed the characteristic particle size to be its diameter (D) and according to the solutions of the anomalous diffraction theory, the particular absorption efficiencies can be expressed as follows:

— for spherical particles (van de Hulst, 1981):

$$Q_a = 1 + 2 \frac{\exp(-4\pi n_w l_p \lambda^{-1} D)}{4\pi n_w l_p D \lambda^{-1}} + 2 \frac{\exp(-4\pi n_w l_p \lambda^{-1} D) - 1}{(4\pi n_w l_p D \lambda^{-1})^2} \tag{20}$$

— for randomly oriented very thin circular cylinders ("infinite" cylinders) (Fournier and Evans, 1996):

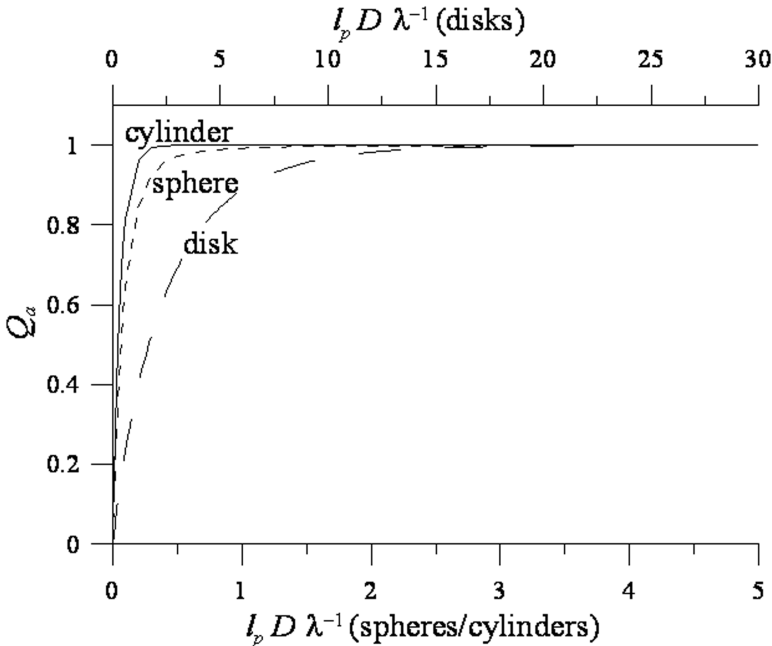$$Q_a = 1 - \exp(-4\pi n_w l_p \lambda^{-1} D) \tag{21}$$

Figure 1. Absorption efficiency factor (Q_a) for spherical, randomly oriented very thin cylindrical particles and flat disks calculated on the basis of anomalous diffraction approximation formulas (Eqs. 20–22).

— for randomly oriented very thin circular disks (Jonasz and Fournier, 2007):

$$Q_a = 1 - 2E_3(4\pi n_w \tau l_p \lambda^{-1} D) \tag{22}$$

where E_3 is the third-order exponential integral and τ is the ratio between the value of a particle's thickness and its diameter (the aspect ratio), τ was assumed to be 0.015.

The value of the absorption efficiency increases monotonically from 0 with increasing particle diameter. Initially the increase is linear ($Q_a \sim l_p \lambda^{-1} D$), and approaches 1 in the infinity. The rate of the increase of the values of Q_a is significantly different among particles of various shapes (Fig. 1). It can be explained by the fact that the magnitude of light absorption depends on the mean geometrical ray path length inside a particle. When particles of considered shapes have the same diameter, this length, which can be roughly approximated as the ratio of the particle volume to its projected area (Bryant and Latimer, 1969), is the longest in the case of cylinders and the shortest for disks. Therefore, for cylinders Q_a approaches 1 very fast, whereas for disks the increase is the slowest (Fig. 1).

The aspect ratio for each particles' shape was kept constant. Therefore, in Eq. 19 describing the relative absorption it only matters that the particles' surface area is proportional to D^2. Moreover, in the case of very long cylinders Q_a does not depend on the aspect ratio (Eq. 21), which has to be sufficiently large to use Eq. 21, and that is why it did not have to be specified.
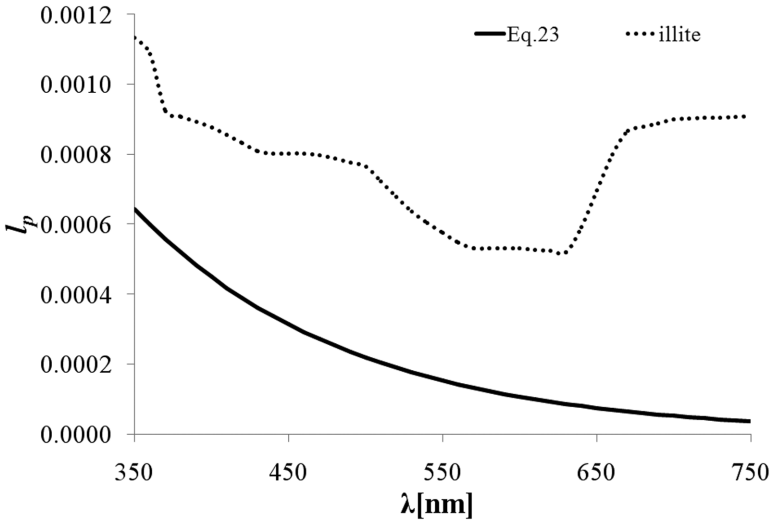
Figure 2. The spectra of the imaginary part of the refractive index (relative to water).

Two functions describing the spectra of the imaginary part of the refractive index l_p were applied (Fig. 2). The first one (solid line in Fig. 2) was taken from Stramski *et al.* (2001) and Woźniak and Stramski (2004) who simulated the spectrum of l_p of detritus and mineral particles in the Sargasso Sea in a following way:

$$l_p = 0.007954 \exp(-0.007186\lambda). \tag{23}$$

The second spectrum (dotted line in Fig. 2) was chosen to have different shape and values of l_p. It was taken from literature (Woźniak and Dera, 2007 who cited the data of Egan and Hilgeman, 1979) and describes a spectrum of l_p of illite which can possibly be an important mineral constituent of clay suspension. It was not our aim to simulate the absorption properties of natural assemblages of particles and chosen spectra of l_p should be treated only as examples, although adequate for the purpose of this study.

The magnitude of the absorption coefficients for respective wavelengths were estimated with a 10-nm step. The calculations were performed for particle assemblages with power-law size distribution (Eq. 1) with the exponent k ranging from 2 to 6. The integrals in Eq. 19 were calculated numerically using the trapezoidal method with a 0.001-μm integration step. The value of D_{min} was assumed to be 0.2 μm. This value is treated as a common operational cutoff between dissolved and particulate matter, which are separated using filters of that pore size (e.g. Stramski *et al.*, 2004; Clavano *et al.*, 2007). This division between particulate and dissolved matter should be considered only as conventional because there are some kinds of particles (e.g. colloids and bacteria) whose sizes are smaller (e.g. Stramski *et al.*, 2004; Stramski and Woźniak, 2005). The chosen magnitude of D_{min} fulfills the condition in Eq. 11 for every considered Q_a and l_p. The values of D_{max}

ranged from 20 to 5000 μm. The highest value of the upper limit of the particle sizes is extremely large as for natural marine conditions. The number concentration of such particles is very low and practically has no influence on the particulate absorption. However, the choice of such a large value of D_{max} enables using Eqs. 13–15 and their approximation (Eq. 18). For spherical and cylindrical particles, even in the case of the lowest values of l_p (Eq. 23) $Q_a(D_{max})$, is close to 1. In order to fulfill this condition for disks the value of D_{max} should be higher than 5000 μm.

The values obtained numerically basing on ADA (Eq. 19) will be a reference to the approximation presented in Eq. 18. The exponent δ in Eq. 18 was determined by means of the least square method after logarithmic transformation:

$$\ln\left[\frac{a_p(\lambda)}{a_p(350)}\right] = \delta\left\{\ln\left(\frac{l_p}{\lambda}\right) - \ln\left[\frac{l_p(350)}{350}\right]\right\}. \tag{24}$$

The component $\ln\lfloor l_p(350)/350 \rfloor$ was assumed to be known thus the relative value of the absorption coefficient $a(\lambda)/a(350)$ was normalized to 1 at 350 nm. The goodness of fit of the approximation (Eq. 18) to the exact ADA results (Eq. 19) was verified by means of two measures: (i) the coefficient of determination R^2 being the squared Pearson's correlation coefficient calculated during the linear regression analysis of Eq. 24 and (ii) the average root-mean-squared (rms) difference between the approximated relative absorption data (Eq. 18), obtained with the use of previously determined delta value, and these calculated using ADA (Eq. 19) divided by the average value of $a(\lambda)/a(350)$. The determination coefficient was used to estimate how well the regression line (Eq. 18) represents the data (Eq. 19). Whereas rms provides the information on the likely percentage error of the approximation.

b. Results

We started the analysis of the approximation of the particle absorption spectra based on Eq. 18 for a wide range of particle diameters, that is expanding from 0.2 to 5000 μm with exponential l_p. For spherical particles, the shape of the spectrum calculated numerically with the use of ADA (Eq. 19) changed from a convex ($k < 3$) through almost linear ($k = 3$) to a concave ($3 < k$) function (dots in Fig. 3a). When the l_p spectrum is a concave function and the exponent δ is positive, a convex spectrum of absorption cannot be reproduced by Eq. 18. Therefore in this case the approximation can only reproduce the character of the absorption spectral shape for $3 < k$ which is confirmed by high values of the coefficient of determination ($0.95 < R^2$) and low rms values. The goodness of fit increases with increasing k, which is also true for particles with other shapes (Fig. 4). Using Eq. 18 gives better results for the second function of the refractive index (illite) (Fig. 3b, Fig. 4) which is characterized by higher values. If the interval of particles' size is sufficiently wide, the absorption spectrum can be determined on the basis of Eq. 12 and its particular forms (Eqs. 13–15). Fig. 3 (solid lines) also presents the absorption spectra of spherical particles obtained with the use of Eqs. 13 and 14 where $\alpha = 2/3\pi^2 n_w$ and $\beta =$
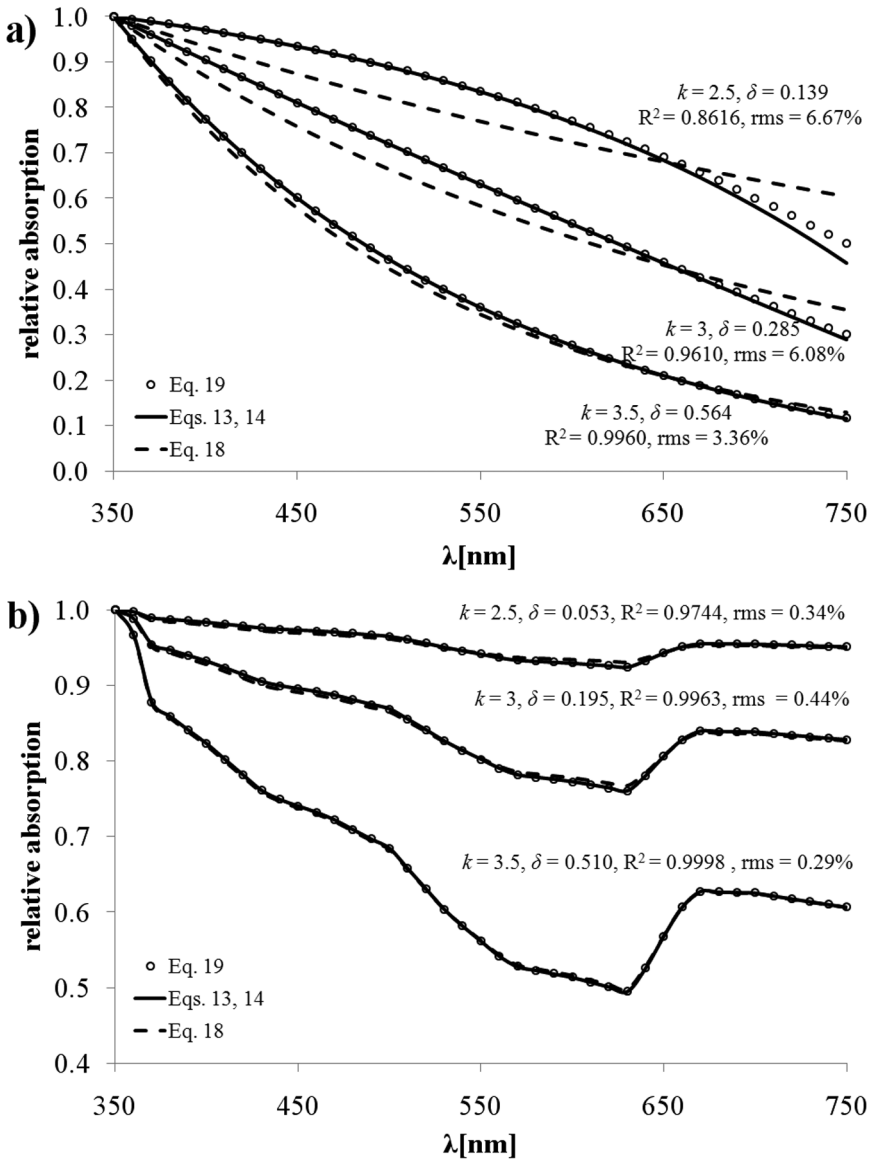
Figure 3. Comparison between the shapes of the absorption spectra obtained on the basis of Eq. 19 (dots), Eqs. 13 and 14 (solid line) and approximated by Eq. 18 (dotted line) of assemblages of spherical particles with power PSD (Eq. 1) for different exponent (k) with diameters ranging from 0.2 to 5000 μm and for two spectra of the imaginary part of the refractive index: (a) exponential and (b) illite. R^2 and rms describe the goodness of fit of the approximation (Eq. 18) to the exact ADA results (Eq. 19).
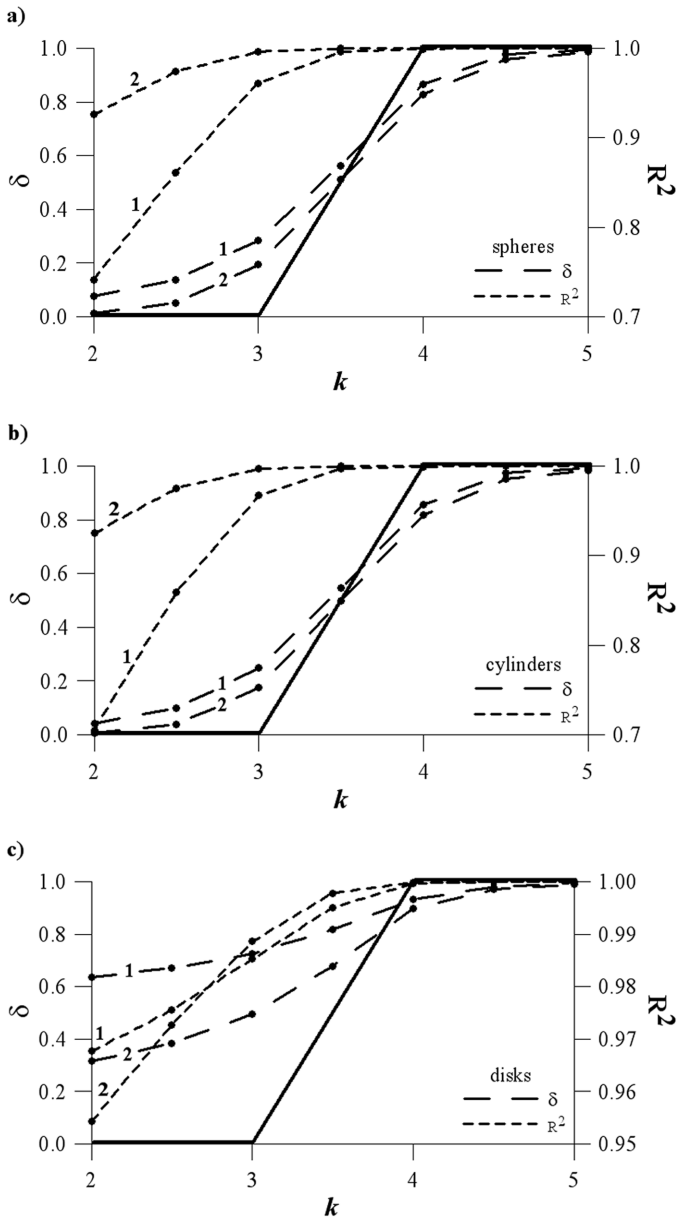
Figure 4. Exponents of the power function approximation of the relative absorption spectra (Eq. 18) within the particles' diameter range 0.2–5000 μm calculated for the particle absorption spectral dependence for exponential (1) and illite (2) l_p, for chosen values of k (Eq. 1) and various particles' shapes: (a) spheres, (b) infinite cylinders and (c) disks. R^2 describes the goodness of fit of the approximation (Eq. 18) to the exact ADA results (Eq. 19). Solid line presents the asymptotic solution (Eq. 17).

$\pi/4$, and $\gamma_o = a_p\,(\lambda_o = 350)/m$ was calculated numerically using ADA. It can be clearly seen that this solution accurately describes the spectral shape of absorption of spheres in the considered range of diameters for both l_p spectra (Fig. 3). For exponential l_p and $k = 2.5$ some slight differences can be noted between estimated (Eq. 13) and numerically calculated values (Eq. 19) of the relative absorption coefficient in the long-wave part of the spectrum (Fig. 3a). This results from the fact that for low values of l_p ($=0.0000364$ at 750 nm) and $D_{\max} = 5000$ μm the value of $Q_a \approx 0.9$ and is too low to fulfill quite satisfactorily the condition that the absorption cross section equals the particle's geometrical cross section.

For a wide range of particles' diameters the exponents δ in Eq. 18 should be similar to the asymptotic values in Eq. 17 describing the absorption spectra for an infinitely large diameter range. Such a situation occurs in the case of spherical and cylindrical particles (Fig. 4a, 4b). Whereas for thin disks and $k \leq 3$ the values of δ are much higher than the asymptotic one, which in this case equals 0 (Fig. 4c). Considering all assumed particle shapes, the increase in the values of the absorption efficiency (Q_a) with increasing particle diameter of disk-shaped particles is the slowest (Fig. 1), and most of Q_a values are relatively small. The absorption spectra of these particles can be approximated by Eq. 18 very well ($0.95 < R^2$) even if $k < 3$. The courses of the dependency between δ and k will tend to the asymptotic one when for $3 < k$ the value of $D_{\min}$ is smaller, because in this case it plays the deciding role (see Section 2), and for $k \leq 3$ the value of $D_{\max}$ is higher.

In the case of narrower particle diameter ranges we arbitrarily set the largest value of the maximum diameter to be 1000 μm (1 mm). It is alleged by some authors that 1000 μm is the upper limit of the diameter of particles which distinctly contribute to light attenuation in sea water (e.g. Jonasz and Fournier, 2007). There were also three lower values of $D_{\max}$ taken into computation; 20, 100, and 500 μm. In most considered cases the absorption spectra were approximated by Eq. 18 very well (Fig. 5). The approximation appeared the weakest for low k, e.g. 2, for cylinders and spheres when the absorption spectra could be described reasonably only in the case of relatively narrow particle diameter ranges (0.2–20 μm and 0.2–100 μm) (Fig. 6). In the assemblages dominated by fine particles caused either by increasing the value of k or lowering the value of $D_{\max}$ the exponent δ is very close to 1, which stays in agreement with the dependency $a_p \sim l_p\lambda^{-1}$. Together with an increase in the particles' diameter interval the value of the exponent decreases, which is caused by the increasing impact of larger particles. Accounting for these results one should be careful when fixing the upper limit of particles' size in modeling the absorption spectra. For PSDs with $k \leq 3$ the value of δ tends to 0 when $D_{\max}$ increases (Fig. 5). For higher values of k, e.g. 4, the variability in δ is the strongest for spheres and cylinders up to $D_{\max} = 500$ μm. Then δ reaches a constant value which is characteristic for the particles' size interval ($0.2 - \infty$ μm). Whereas for disks δ still slightly decreases. For $5 \leq k$ the exponent δ is almost constant (close to 1) irrespective of the width of the particles' diameter ranges. For example, in the case of cylindrical particles and $k = 6$, $\delta = 0.993$ ($0.9999 < R^2$) and 0.995 ($0.9999 < R^2$) for illite and exponential l_p, respectively. Like for
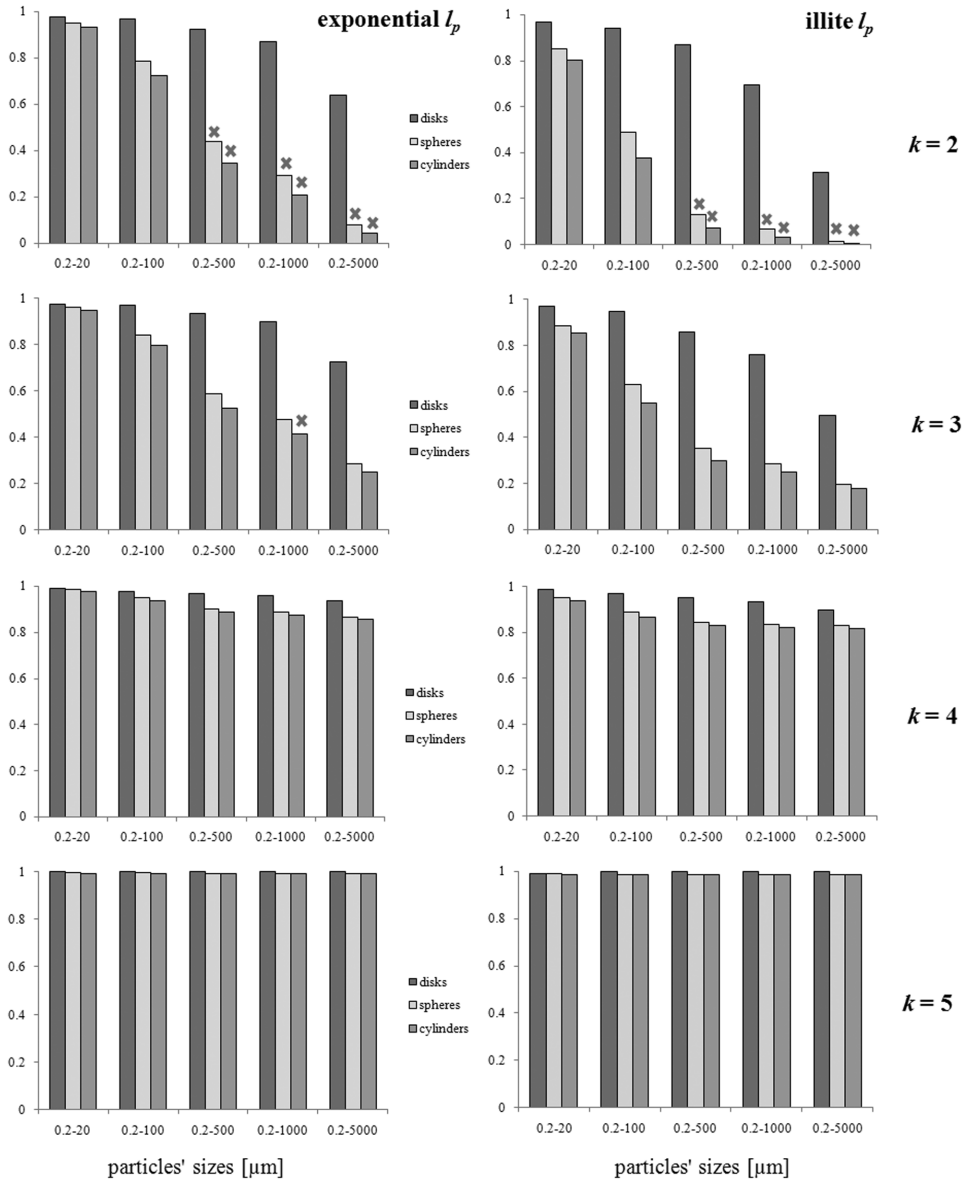
Figure 5. Values of the exponent δ calculated for the particle absorption spectral dependence (Eq. 18) for power-law PSD (Eq. 1) for chosen values of k, various intervals of particles' diameters and shapes (spheres, infinite cylinders and disks). Crosses indicate the cases when $0.95 < R^2$.

the absorption by particles with a wide range of diameters, the approximation is best in the case of disks and generally the goodness of fit improves with an increasing value of k.

Summarizing, the accuracy of the approximation (Eq. 18) is at the same time related to
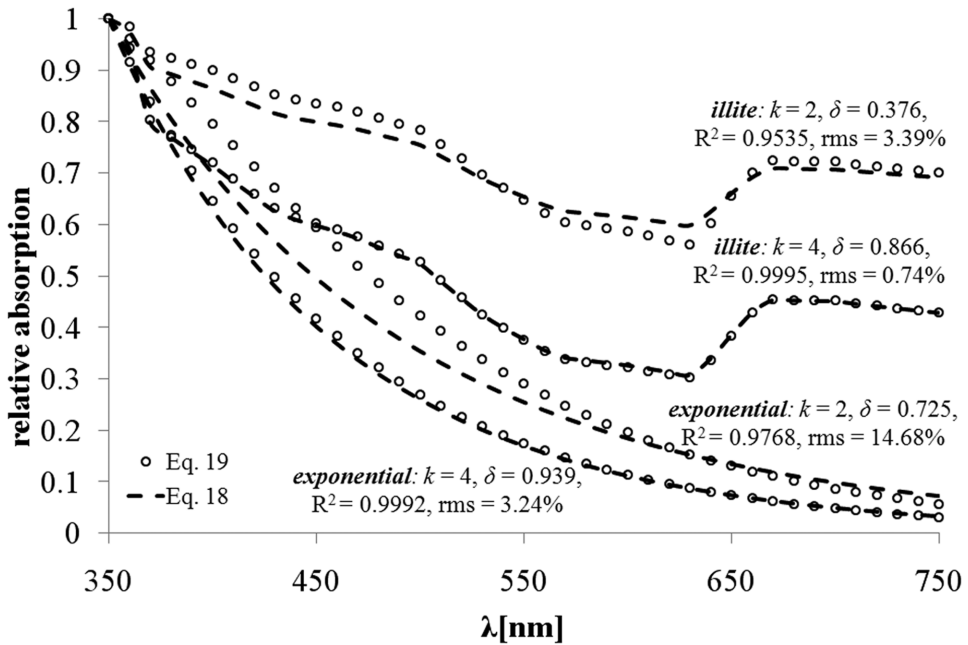
Figure 6. Relative absorption spectra obtained on the basis of Eq. 19 (dots) and approximated by Eq. 18 (dotted line) of assemblages of cylindrical particles with power-law PSD (Eq. 1) for different exponent (k) with diameters ranging from 0.2 to 100 μm and for illite and exponential spectra of the imaginary part of the refractive index. R^2 and rms describe the goodness of fit of the approximation (Eq. 18) to the exact ADA results (Eq. 19).

the courses of the $Q_a(l_p\lambda^{-1}D)$ function (Fig. 1) and the PSD slope. Best fits were obtained: (i) when the values of Q_a mostly contributing to the magnitude of the absorption coefficient result from the presence of relatively small particles or (ii) the particle size range were wide enough that the absorption spectrum was close to the asymptotic one (Eq. 17). In an "intermediate" situation the accuracy of Eq. 18 can be lower, as for an assemblage of cylindrical particles with diameters ranging from 0.2 to 1000 μm, exponential l_p and $k = 3$ (Fig. 5).

4. Interpretation of nonalgal particles' absorption spectra

a. Slope coefficient

The relationship between the marine particles' absorption coefficient and the light wavelength expressed with a power function of $l_p\lambda^{-1}$ (Eq. 18) resembles the dependency used to describe the absorption coefficient spectra of atmospheric aerosols (Angstrom, 1929). It is commonly used today and is written in the following way:

$$a_{aer} \sim \lambda^{-AAE} \qquad (25)$$

where the positive constant exponent is nowadays called the Absorption Angstrom Exponent (*AAE*) (Bergstrom *et al.,* 2007).

Despite the fact that the imaginary part of the refractive index of aerosols is not involved in Eq. 25, its variability can influence the magnitude of *AAE*. For some small particles, a value of *AAE* lower than 1 can result from an increase in the l_p value with the wavelength (Bergstrom *et al.,* 2007). In some cases the Angstrom formula can approximate quite well the absorption spectra of marine particles presented in the previous section, i.e. when $3 < k$ and l_p was described by an exponential function (Eq. 23).

Unlike atmospheric aerosols, the absorption spectra of marine nonalgal suspended matter, consisting of both organic (detritus) and mineral particles in different proportions, are usually expressed with the use of an exponential function:

$$a_p(\lambda) = a_p(\lambda_o) \exp[-s(\lambda - \lambda_o)] \tag{26}$$

where a constant positive coefficient s [nm^{-1}] describes the rate of the absorption decrease with increasing wavelength.

Various empirical studies showed that the values of the slope coefficient (s) range approximately from 0.0024 to 0.019 nm^{-1} (Roesler *et al.,* 1989; Bricaud and Stramski, 1990; Bowers and Binding, 2006; Woźniak and Dera, 2007). When the absorption spectrum of an assemblage of particles with a power-law PSD is a distinctly decreasing function, then it could be expected that the values of l_p also should decrease with increasing wavelength. At the present state of knowledge on the physical properties of marine particles it is considered that the visible l_p spectrum of nonalgal particles is a decreasing function and generally has an exponential character (e.g. Stramski *et al.,* 2001). Theoretical simulations of the spectra of l_p for various chemical classes, accounting for complex internal structures and different morphological features, seem to confirm this fact (Woźniak and Dera, 2007). Let us assume that the spectrum of the imaginary part of the refractive index is described by an exponential function: $l_p \sim \exp(-p\lambda)$, where p [nm^{-1}] is a positive constant coefficient. Then the slope coefficient (s) can be determined with the use of the logarithm of Eq. 18:

$$\ln a_p(\lambda) = \ln a_p(\lambda_o) - \delta p(\lambda - \lambda_o) + \delta \ln(\lambda_o \lambda^{-1}) \tag{27}$$

and the logarithm of Eq. 26:

$$\ln a_p(\lambda) = \ln a_p(\lambda_o) - s(\lambda - \lambda_o). \tag{28}$$

After comparing the above equations the slope coefficient can be expressed as follows:

$$s = \delta \left[p - \frac{\ln(\lambda_o \lambda^{-1})}{\lambda - \lambda_o} \right]. \tag{29}$$

The factor $\ln(\lambda_o \lambda^{-1})$ has the course close to the linear function $c(\lambda - \lambda_o)$, where c [nm^{-1}] is a negative constant. With given value of λ_o its value slightly varies depending on

the considered range of the wavelength. If this linear approximation is taken into account, the magnitude of the slope coefficient s can be easily interpreted by means of the approximate relation:

$$s = \delta(p - c). \tag{30}$$

To illustrate this we used Eq. 30 to estimate the value of s of the absorption spectrum of spheres with diameters' ranging from 0.2 μm to 5000 μm and $k = 4$. In the case of wavelengths ranging from 350 ($= \lambda_o$) to 750 nm, c is equal to -0.00207 nm^{-1} (R^2 = 0.9751), $p = 0.007186$ nm^{-1} (Eq. 23) and the estimated value of $\delta = 0.866$ (R^2 = 0.9996) (Fig. 5). The value of the slope coefficient determined on the basis of Eq. 30 equals 0.008016 nm^{-1}. This result is very close to that estimated directly from the absorption spectrum by means of linear regression (Eq. 28), that is 0.008019 nm^{-1} (R^2 = 0.9998). Actually, the slope coefficient s represents the average value of the local absorption slope coefficient defined as follows:

$$s(\lambda) = -\frac{1}{a_p}\frac{\partial a_p}{\partial \lambda}. \tag{31}$$

According to Eq. 18 $s(\lambda)$ spectrum is mainly influenced by $-\dfrac{d \ln l_p}{d\lambda} + \lambda^{-1}$. The strongest variability in the values of the slope coefficient can be caused by the changes of l_p. This is clearly seen on the absorption spectra of illite particles (Fig. 3b, Fig. 6). Nonexponential behavior of l_p can be the reason for the occurrence of a "shoulder" between 450 and 550 nm in the measured absorption spectra of suspended matter dominated by mineral particles (e.g. Bowers and Binding, 2006). If l_p or the derivative of its logarithm is constant, the value of $s(\lambda)$ will decrease with increasing wavelength only because of λ^{-1}.

b. Comparison with published results of Mie calculations

Stramski *et al.* (2001) numerically simulated the spectra of the average absorption cross sections of detrital and mineral particles with power-law size distribution for $k = 4$ and exponential l_p (Eq. 23) applying Mie solution for homogeneous spherical particles. Later Woźniak and Stramski (2004), using the same approach, calculated the mineral mass specific absorption coefficient for other values of k and one additional l_p spectrum. The absorption cross section as well as the mass specific absorption are proportional to the particles' absorption coefficient itself. One can note that the spectral shape of the absorption (Fig. 4a, b from Woźniak and Stramski, 2004) and the imaginary part of the refractive index (Fig. 2c from Woźniak and Stramski, 2004) are similar. However, for the same l_p and k and different constant values of the real part of the refractive index (n_p) the absorption spectra are slightly shifted against themselves (Woźniak and Stramski, 2004). It means that the spectral shape of particle absorption depends mostly on l_p. Besides, when considering different types of particulate matter the dependency of n_p on the wavelength is relatively

Table 1. The values of coefficients δ (exponent of the power function of $l_p \lambda^{-1}$ in Eq. 18) and s^a (in the exponential dependency given by Eq. 26) of visible (350–750 nm) absorption spectra of spherical particles (0.05–500 μm) with power-law PSD (Eq. 1) of various slopes (k) calculated on the basis of Mie solution (Woźniak and Stramski, 2004) for $n_p = 1.18$ and ADA; (1) exponential l_p (Eq. 23), (3) Sahara dust l_p. R^2 and rms describe the goodness of fit of the approximations to the ADA[b] and Mie results.

		Mie						ADA					
k	l_p	δ	R^2	rms	$s \cdot 10^2$	R^2	rms	δ	R^2	rms	$s \cdot 10^2$	R^2	rms
3.2	(1)	0.689	0.9894	11.65%	0.626	0.9933	8.74%	0.713	0.9883	12.79%	0.647	0.9925	10.59%
	(3)	0.327	0.9983	1.28%	-	-	-	0.333	0.9984	1.25%	-	-	-
4	(1)	0.944	0.9999<	2.18%	0.855	0.9995	5.46%	0.935	0.9997	3.91%	0.848	0.9999<	0.97%
	(3)	0.820	0.9997	1.02%	-	-	-	0.826	0.9999	1.17%	-	-	-
4.8	(1)	1.029	0.9995	6.57%	0.932	0.9982	11.76%	0.998	0.9999<	0.15%	0.904	0.9996	4.58%
	(3)	0.999	0.9999	0.93%	-	-	-	0.978	0.9999<	0.64%	-	-	-

[a]The values of coefficients δ and s were determined by means of two-parameter linear regression, i.e. the reference wavelength was not fixed, after appropriate logarithmic transformation of Eqs. 18 and 26.

[b]In the case of ADA the regression was performed for the relative absorption spectra, but all presented parameters would be the same if calculations were performed for the absolute absorption coefficient values.

weak (e.g. Woźniak and Dera, 2007). Since ADA expresses Q_a as a function of l_p, one can suppose that the spectral shape of absorption suggested by Eq. 18 derived from consideration based on ADA can be a good approximation in the case of cited Mie calculations as well. This idea was tested basing on the goodness of fit of the power function of $l_p \lambda^{-1}$ to the spectra of the mass specific absorption coefficients presented graphically by Woźniak and Stramski (2004) for two different spectra of l_p. The first one is as in Eq. 23 (Fig. 1) whereas the second one, with values higher by one order of magnitude (~0.01), is based on data for Saharan dust. In the latter case l_p decreases approximately in an exponential manner between 350 and 600 nm and for the longer wavelengths the spectrum is flat. The mass specific absorption coefficients and Saharan l_p values taken by us into calculations were obtained through digitalization of proper graphs (Fig. 2c and 4b from Woźniak and Stramski, 2004). The use of digitalized values only slightly influenced the results of the analysis. For example, for $k = 4$ and exponential l_p we calculated the slope coefficient s (Eq. 26) to be 0.00855 nm^{-1} (Table 1) whereas its original value determined by Stramski *et al.* (2001) varied between 0.00846 and 0.00847 nm^{-1} depending on the magnitude of constant n_p.

According to our estimation, in most cases the absorption coefficient approximated by a power function of $l_p \lambda^{-1}$ explained at least 99% of its spectral variability calculated with Mie theory. In the case of weakly absorbing particles (exponential l_p spectrum) and low values of k (e.g. $k = 3.2$) the goodness of fit of this approximation was the worst, which was indicated by the highest values of the rms error (Table 1). It is also true in the case of the anomalous diffraction approximation, which is consistent with the results described in the previous section

(see Fig. 3a, Fig. 6). When $k = 4.8$ the value of δ determined by the Mie solution was slightly higher than 1 (Table 1) which is the maximum value of the exponent predicted basing on ADA. The most probable reason for this result is that according to this exact solution the absorption coefficient in the Rayleigh absorption limit does not depend linearly on the imaginary part of the refractive index (van de Hulst, 1981; Bohren and Huffman, 1983). Relative differences, with respect to the Mie results, between the values of δ and s obtained on the basis of Mie and ADA computation did not exceed 3.5%. Based on the similarity in the magnitudes of both these parameters, the absorption spectrum slope coefficient s determined by means of Mie solutions can also be interpreted by the relationship given in Eq. 30.

5. Conclusions

Natural marine particles are characterized by a large diversity of shapes and complex physical and chemical structures. Exact solutions to the light attenuation are usually very complicated even for model particles with distinctly simplified properties. The anomalous diffraction approach to the light absorption, despite neglecting the reflection and refraction when considering interaction between the light and the particles, seems to enhance an approximate but effective analysis and provides an interpretation of their absorption spectra shape. We showed that for power-law particle size distribution some solutions and approximations based on ADA can be related to the homogeneous particles of theoretically any shape. The key parameter determining the shape of the particles' absorption is $l_p\lambda^{-1}$. A power function of $l_p\lambda^{-1}$ approximates the absorption dependency on l_p spectrum in the most simple manner being in fact a modification of the classical Angstrom law (Eq. 25). Despite we focused on non-algal particles it can be expected that this relation can be applied in the case of the phytoplankton absorption as well. In particular, the obtained results can be useful in various studies involving the absorption coefficient as an important factor.

REFERENCES

Aas, E. 1996. Refractive index of phytoplankton derived from its metabolite composition. J. Plankton Res., *18,* 2223–2249.

Angstrom, A. 1929. On the atmospheric transmission of sun radiation and on dust in the air. Geografiska Annaler, *11,* 156–166.

Babin, M., A. Morel, V. Fournier-Sicre, F. Fell and D. Stramski. 2003. Light scattering properties of marine particles in coastal and open ocean waters as related to the particle mass concentration. Limnol. Oceanogr., *48,* 843–859.

Bader, H. 1970. The hyperbolic distribution of particles sizes. J. Geophys. Res., *75,* 2822–2830.

Baird, M. E. 2003. Numerical approximations of the mean absorption cross-section of a variety of randomly oriented microalgal shapes. J. Math. Biol., *47,* 325–336.

Barnard, H., W. S. Pegau and J. R. V. Zaneveld. 1998. Global relationships of the inherent optical properties of the oceans. J. Geophys. Res., *103*(C11), 24955–24968.

Bergstrom, R. W., P. Pilewskie, P. B. Russell, J. Redemann, T. C. Bond, P. K. Quinn and B. Sierau. 2007. Spectral absorption properties of atmospheric aerosol. Atmos. Chem. Phys., *7,* 5937–5943.

Bohren, C. F. and D. R. Huffman. 2004. Absorption and Scattering by Small Particles, Wiley—VCH Verlag GmbH&Co. KGaA, 530 pp.

Boss, E., M. S. Twardowski and S. Herring. 2001. Shape of particulate beam attenuation spectrum and its inversion to obtain the shape of the particulate size distribution. Appl. Opt., *40,* 4885–4893.

Bowers, D. G. and C. E. Binding. 2006. Optical properties of mineral suspended particles in the sea: A review and synthesis. Estuar. Coast. Shelf Sci., *67,* 219–230.

Bricaud, A. and A. Morel. 1986. Light attenuation and scattering by phytoplanktonic cells: a theoretical modeling. Appl. Opt., *25,* 571–580.

Bricaud, A. and D. Stramski. 1990. Spectral absorption coefficients of living phytoplankton and nonalgal biogenous matter: a comparison between the Peru upwelling area and the Sargasso Sea. Limnol. Oceanogr., *35,* 562–582.

Bryant, F. D. and P. Latimer. 1969. Optical efficiencies of large particles of arbitrary shape and orientation. J. Colloid Interface Sci., *30,* 291–304.

Buonassissi, C. J. and H. M. Dierssen. 2010. A regional comparison of particle size distributions and the power law approximation in oceanic and estuarine surface waters. J. Geophys. Res., *115,* C10028, doi:10.1029/2010JC006256.

Carder, K. L., G. F. Beardsley, Jr. and H. Pak. 1971. Particle size distributions in the eastern equatorial Pacific. J. Geophys. Res., *76,* 5070–5077.

Chang, G., A. Barnard and J. R. V. Zaneveld. 2007. Optical closure in a complex coastal environment: particle effects. Appl. Opt., *46,* 7679–7692.

Chang, G. C. and T. D. Dickey. 2004. Coastal ocean optical influences on solar transmission and radiant heating rate. J. Geophys. Res., *109,* C01020.

Clavano, W. R., E. Boss and L. Karp-Boss. 2007. Inherent optical properties of non-spherical marine-like particles—from theory to observations. Oceanogr. Mar. Biol. Annu. Rev., *45,* 1–38.

Dera, J. 2003. Fizyka morza. PWN, 544 pp (in Polish).

Doxaran, D., K. Ruddick, D. McKee, B. Gentili, D. Tailliez, M. Chami and M. Babin. 2009. Spectral variations of light scattering by marine particles in coastal waters, from the visible to the near infrared. Limnol. Oceanogr., *54,* 1257–1271.

Duysens, L. N. M. 1956. The flattening of the absorption spectrum of suspensions as compared to that of solutions. Biochim. Biophys. Acta, *19,* 1–12.

Edwards, A. M., T. Platt and D. G. Wright. 2001. Biologically induced circulation at fronts. J. Geophys. Res., *106*(C4), 7081–7095.

Edwards, A. M., D. G. Wright and T. Platt. 2004. Biological heating effect of a band of phytoplankton. J. Mar. Syst., *49,* 89–103.

Egan, W. G. and T. W. Hilgeman. 1979. Optical Properties of Inhomogeneous Materials: Application to Geology, Astronomy, Chemistry, and Engineering, Academic Press, 246 pp.

Fichtenholz, G. M. 1978. Rachunek Różniczkowy i Całkowy II. PWN, 696 pp (in Polish).

Fournier, G. R and B. T. N. Evans. 1994. Analytic approximation to randomly oriented spheroid extinction. Appl. Opt., *33,* 5796–5804.

—— 1996. Approximations to extinction from randomly oriented circular and elliptical cylinders. Appl. Opt., *35,* 4271–4282.

Gordon, H. R., O. B. Brown and M. M. Jacobs. 1975. Computed relationships between the inherent and apparent optical properties of a flat homogenous ocean. Appl. Opt., *14,* 417–427.

Harris, J. E. 1977. Characterization of suspended matter in the Gulf of Mexico. II: Particle size distribution of suspended matter from deep water. Deep-Sea Res., *24,* 1055–1061.

Jerlov, N. G. 1976. Marine Optics, Elsevier, 120 pp.

Jonasz, M. and G. Fournier. 1996. Approximation of the size distribution of marine particles by a sum of log-normal functions. Limnol. Oceanogr., *41,* 744–754.

—— 2007. Light Scattering by Particles in Water, Academic Press, Elsevier, 704 pp.

Kirk, J. T. O. 1975. A theoretical analysis of the contribution of algal cells to the attenuation of light within natural waters. II. Spherical cells. New Phytol., *75,* 21–36.

—— 1976. A theoretical analysis of the contribution of algal cells to the attenuation of light within natural waters. III. Cylindrical and spheroidal cells. New Phytol., *77,* 341–358.

—— 1984. Dependence of relationships between inherent and apparent optical properties of water on solar altitude. Limnol. Oceanogr., *29,* 350–356.

—— 1991. Volume scattering function, average cosines and the underwater light field, Limnol. Oceanogr., *36,* 455–467.

Kostadinov, T. S., D. A. Siegel and S. Maritorena. 2009. Retrieval of the particle size distribution from satellite ocean color observations. J. Geophys. Res., *114,* C09015, doi:10.1029/2009JC005303.

Latimer, P. 1984. A wave-optics effect which enhances light absorption by chlorophyll in vivo. Photochem. Photobiol., *40,* 193–199.

Lewis, M. R., J. J. Cullen and T. Platt. 1983. Phytoplankton and thermal structure in the upper ocean. Consequences of non-uniformity in chlorophyll profile. J. Geophys. Res., *88,* 2565–2570.

Liu, Y., W. P. Arnott and J. Hallett. 1998. Anomalous diffraction theory for arbitrarily oriented finite circular cylinders and comparison with exact T-matrix results. Appl. Opt., *37,* 5019–5030.

McCave, I. N. 1984. Size spectra and aggregation of suspended particles in the deep ocean. Deep-Sea Res., *31,* 329–352.

Mishchenko, M. I., L. D. Travis and A. L. Lacis. 2002. Scattering, Absorption, and Emission of Light by Small Particles, Cambridge University Press, 480 pp.

Mitchell, B. G., 1990. Algorithms for determining the absorption coefficient for aquatic particulates using the quantitative filter technique, Ocean Optics *10,* Proc. SPIE *1302,* 137–148.

Mitchell, B. G., A. Bricaud, K. Carder, J. Cleveland, G. M. Ferrari, R. Gould, M. Kahru, M. Kishino, H. Maske, T. Moisan, L. Moore, N. Nelson, D. Phinney, R. A. Reynolds, H. Sosik, D. Stramski, S. Tassan, C. Trees, A. Weidemann, J. D. Wieland and A. Vodacek. 2000. Determination of spectral absorption coefficients of particles, dissolved material and phytoplankton for discrete water samples, *in* Ocean Optics Protocols For Satellite Ocean Color Sensor Validation, Revision 2, G. S. Fargion, J. L. Mueller and C. R. McClain, eds., NASA Technical Memorandum 2000–209966, Chapter 12, 125–153.

Mobley, C. D. 1994. Light and Water: Radiative Transfer in Natural Waters, Academic Press, 592 pp.

Morel, A. 1973. The scattering of light by sea water. Experimental results and theoretical approach, *in* Optics of the Sea, Interface and In-Water Transmission and Imaging, AGARD lecture Series, *61,* 161 pp.

—— 1994. Optics from the Single Cell to the Mesoscale, *in* Ocean Optics, R. W. Spinrad, ed., Oxford University Press, 93–106.

Morel, A. and A. Bricaud. 1981. Theoretical results concerning light absorption in a discrete medium, and application to specific absorption of phytoplankton. Deep-Sea Res., *28,* 1375–1393.

Ohlmann, J. C., D. A. Siegel and C. D. Mobley. 2000. Ocean radiant heating. Part I: Optical influences. J. Phys. Oceanogr., *30,* 1833–1849.

Oschlies, A. 2004. Feedbacks of biotically induced radiative heating on upper-ocean heat budget, circulation, and biological production in a coupled ecosystem-circulation model. J. Geophys. Res., *96,* 14947–14957.

Paramonov, L. E. 1994. On optical equivalence of randomly oriented ellipsoidal and polydisperse spherical particles. The extinction, scattering and absorption cross sections. Optika i Spektroskopyia, *77,* 660–663 (in Russian).

Quirantes, A. and S. Bernard. 2004. Light scattering by marine algae: two-layer spherical and non-spherical models. J. Quant. Spectrosc. Ra., *89,* 311–321.

Ramp, S. R., R. W. Garwood, C. O. Davis and L. R. Snow. 1991. Surface heating and patchiness in

the coastal ocean off California during a wind relaxation event. J. Geophys. Res., *96,* 14947–14957.

Risovic, D. 1993. Two-component model of sea particle size distribution. Deep-Sea Res., *40,* 1459–1473.

Roesler, C. S., M. J. Perry and K. L. Carder. 1989. Modeling *in situ* phytoplankton absorption from total absorption spectra in productive inland marine waters. Limnol. Oceanogr., *34,* 1510–1523.

Sheldon, R. W., A. Prakash and W. H. Sutcliffe Jr. 1972. The size distribution of particles in the sea. Limnol. Oceanogr., *17,* 327–340.

Simpson, J. J. and T. D. Dickey. 1981. The relationship between downward irradiance and upper ocean structure. J. Phys. Oceanogr., *11,* 309–323.

Stramska, M. and T. D. Dickey. 1993. Phytoplankton bloom and the vertical thermal structure of the upper ocean. J. Mar. Res., *51,* 819–842.

Stramski, D., E. Boss, D. Bogucki and K. J. Voss. 2004. The role of the seawater constituents in light backscattering in the oceans. Prog. Oceanogr., *61,* 27–56.

Stramski, D., A. Bricaud and A. Morel. 2001. Modeling the inherent optical properties of the ocean based on the detailed composition of the planktonic community. Appl. Opt., *40*(18), 2929–2945.

Stramski, D. and S. B. Woźniak. 2005. On the role of colloidal particles in light scattering in the ocean. Limnol. Oceanogr., *50,* 1581–356.

Sun, W. and Q. Fu. 1999. Anomalous diffraction theory for arbitrarily oriented hexagonal crystals. J. Quant., Spectrosc. Radiat. Transfer, *63,* 727–737.

Tassan, S. and G. M. Ferrari. 1995. An alternative approach to absorption measurements of aquatic particles retained on filters. Limnol. Oceanogr., *40,* 1358–1368.

Thomas, G. E. and K. Stamnes. 1999. Radiative Transfer in the Atmosphere and Ocean. Cambridge University Press, 546 pp.

Twardowski, M. S., E. Boss, J. B. MacDonald, W. S. Pegau, A. H. Barnard and J. R. V. Zaneveld. 2001. A model for estimating bulk refractive index from the optical backscattering ratio and the implications for understanding particle compositions in Case I and Case II waters. J. Geophys. Res., *C106,* 14129–14142.

Van de Hulst, H. C. 1981. Light Scattering by Small Particles, Dover Publications, 470 pp.

Vickers, G. T. and D. J. Brown. 2001. The distribution of projected area and perimeter of convex, solid particles. Proc. R. Soc. Lond. A, *457,* 283–306.

Volz, F. 1954. Die Optik und Meteorologie der atmosphärischen Trubung. Ber. Dtsch. Wetterdienstes, *2,* 3–47.

Woźniak, S. B. and D. Stramski. 2004. Modelling the optical properties of mineral particles suspended in seawater and their influence on ocean reflectance and chlorophyll estimation for remote sensing algorithm. Appl. Opt., *43,* 3480–3503.

Woźniak, B. and J. Dera. 2007. Light Absorption in Sea Water, Springer, 456 pp.

Yang, P., Z. Zhang, B. A. Baum, H. L. Huang and Y. Hu. 2004. A new look at anomalous diffraction theory (ADT): Algorithm in cumulative-projected area distribution domain and modified ADT. J. Quant. Spectrosc. Ra., *89,* 421–307.

Yentsch, C. S. 1962. Measurement of visible light absorption by particulate matter in the ocean. Limnol. Oceanogr., *7,* 207–217.

Zaneveld, R., A. Barnard and Z. P. Lee. 2006. Why are Inherent Optical Properties Needed in Ocean-Colour Remote Sensing? *in* Remote Sensing of Inherent Optical Properties: Fundamentals, Tests of algorithms, and applications, Z. P. Lee, ed., Reports of the International Ocean-Colour Coordinating Group, No. 5, IOCCG, Dartmouth, Canada, 3–13.